JEE Journal of Ecological Engineering

Journal of Ecological Engineering, 2025, 26(9), 197–204
https://doi.org/10.12911/22998993/204171
ISSN 2299–8993, License CC-BY 4.0

Received: 2025.03.14
Accepted: 2025.06.13
Published: 2025.06.23

Wind induced energy harvesting with an aero-elastic resonator: Effect of the bluff body diameter

Grzegorz Litak[1], Jacek Caban[1*], Sreeja Sadasiavan[1,2], Mariusz Klimek[1], Jerzy Margielewicz[3], Damian Gąska[3]

[1] Faculty of Mechanical Engineering, Lublin University of Technology, ul. Nadbystrzycka 36, 20-618 Lublin, Poland
[2] School of Mechanical Engineering, Vellore Institute of Technology, 632014 Tamil Nadu, India
[3] Faculty of Transport and Aviation Engineering, Silesian University of Technology, ul. Krasińskiego 8, 40-019 Katowice, Poland
* Corresponding author's e-mail: j.caban@pollub.pl

ABSTRACT

Ambient energy harvesting from the airflow environment is defined through an additional mechanical structure exposed to wind force. Using a simplified vortex shedding model, the cylinder was modelled like a bluff body interaction with flowing air. The mechanical resonator was composed of the cylinder attached to the beam with a piezo patch. The vortex shedding on the cylinder was modelled as Van der Pol oscillator. In particular, the effect of cylinder diameter on the output voltage was analysed. The growth of the wind speed interval the top voltage output were reported as a result of the increasing diameter. The uncertainty the power output caused by the uncertain bluff body diameter increased considerably at the upper edge of Vortex Induced Vibration mechanism.

Keywords: energy harvesting system, piezoelectric, flow structure interaction, vortex induced vibration.

INTRODUCTION

The current huge demand for energy is visible in many human activity areas. The use of an alternative power source for various systems and sensors that are part of the equipment of various technical facilities has become very important (Ali et al., 2024; Ambrożkiewicz et al., 2022; Ceponis et al., 2019; Gałęzia et al., 2012; Kindrachuk et al., 2019; Naifar et al., 2024). Energy management in technical facilities has become a very important issue, for example energy management systems in motor vehicles. This resulted from the need to manage the energy generated from fuel and recovered during vehicle operation. Additional systems for energy harvesting systems are instated in the suspension (Chen et al., 2022; Li et al., 2019) and braking system of a vehicle (Gechev et al., 2017; Labuda et al., 2010; Szumska and Jurecki 2022). Thermoelectric energy generators recover energy from the exhaust system (Caban 2021; Wang et al., 2022), while piezoelectric or electromagnetic transducers recover it from mechanical vibrations of the combustion engine (Caban et al., 2024). Other applications include airflow and rotational energy sources (Barta et al., 2022; Ikbal et al., 2025; Naik et al., 2023). The harvested energy can be used for various purposes depending on its size. Some of the energy can be reused to drive vehicles and other smaller energy sources to power selected sensors or micro-sensors (Koszewnik 2024, Nowak et al., 2020). In addition, energy converters can be used in road infrastructure to monitor traffic or weather conditions, monitor the condition of bridge structures, etc. (Bacinskas 2013; Gałęzia et al., 2012; Kilikevicius et al., 2019). Transport is just one of the sectors in which waste energy can be collected. Similar systems can be used in construction, electrical engineering and other sectors. The possibilities offered by converting mechanical vibration energy into electrical energy allow for an increasingly wide range

of applications for such systems (Borowiec et al., 2021; Camut et al., 2023; Nowak and Pietrzakowski 2016; Kim et al, 2023; Yu et al., 2024).

Energy harvesting from ambient vibration can be defined directly on the air-flow environment or through the mechanical structure exposed to the windy conditions. Similarly, energy from see waves and water flow movement can captured and transformed to electrical power. Finally, energy harvesting can be also realized via coupling to vibrating technical systems (Yang et al., 2018; Giri et al., 2022; Friswell et al., 2012; Ma and Zhou 2022). Air flow and mechanical structure interactions are dependent on the bluff body shape. In particular, curved shapes are crucial for vortex induced vibration (VIV) with vortex creation and release at the corresponding surface bends, while inclined shapes lead to the galloping effect involving pressure drop during the flow through variable cross-section and restore force of the spring structure (Giri et al., 2022; Ma and Zhou 2022).

VIV play a main role in excitation of cylindrical bluff bodies in the presence of fairly low air flow speed. Consequently, for such bodies suspended on the elastic spring, there are two characteristic frequencies one coming from vortex shedding and the natural frequency related to mechanical mass-spring system. Matching of these two frequencies defines the resonance conditions. In the mass-spring system, which is linear, the natural frequency is fixed but the nonlinearity in vortex creation and shedding make the shedding frequency and vortex force correlation. Consequently, the resonance conditions are defined in the wind speed interval known as frequency lock region. The dimeter of a cylinder bluff body and the wind speed influence on vortex formation, its evolution and finally shedding frequency. On the other hand, the shedding phenomenon is important for excitation of the bluff body. Energy harvesting from ambient conditions requires the extended efficiency for variable source parameters (Wang et al., 2018; Jung and Seung-Woo 2011; Wang et al., 2020; Li et al., 2024; Navrose and Mittal 2019; Li et al., 2019).

In the present paper, the voltage response to the sweep of wind speed was studied. It should be noted that a closed cylinder on the elastic cantilever beam is subjected to vibrations. The energy transducer is attached to be the elastic beam (Figure 1). Its deformation can produce the power output on the resistor load in the circuit where the electrodes are placed on the piezoelectric.

MATHEMATICAL MODEL

The discussion starts from the system presented in the schematics (Figure 1). The structural equation governing the vibration of the elastically mounted cylinder, enabling transverse vibration in the *x*-direction, is as follows (Li et al., 2024):

$$m\ddot{x} + c\dot{x} + kx - \Theta v = \\ = 0.25\rho U^2\, DLC_{l0}q - 0.5\rho UDLC_{d0}\dot{x} \quad (1)$$

$$\ddot{q} + \beta\omega_s\,(q^2 - 1)\dot{q} + \omega_s^2 q = \frac{A}{D}\ddot{x} \quad (2)$$

$$C_p\dot{v} + \frac{v}{R} + \theta\dot{x} = 0 \quad (3)$$

Where the Equation 1 governs the dynamics of mechanical resonator, the second Equation 2 given by the common Var der Pol form. Here, auxiliary variable q changes constitute modelling vortex dynamics initiating the oscillations of mechanical oscillator structure, and the third Equation 3 is related to the electrical circuit coupled by the piezoelectric to the mechanical oscillator (resonator). Consequently, x is the displacement of the cylinder while v is the voltage output in the resistor of the electrical circuit. L, D and define geometry of the cylindrical bluff body (length and diameter) while m, c and k are inertial, damping and spring properties of the mechanical resonator, respectively. ρ is the air density, U is the wind speed. C_{l0} and C_{d0} are lift and drag coefficients. β and A are fitting parameters (Li et al., 2024) while ω_s and is the approximate shedding frequency. The electrical circuit is defined by the electrical capacity C_p and the ohmic load R, while Θ is the

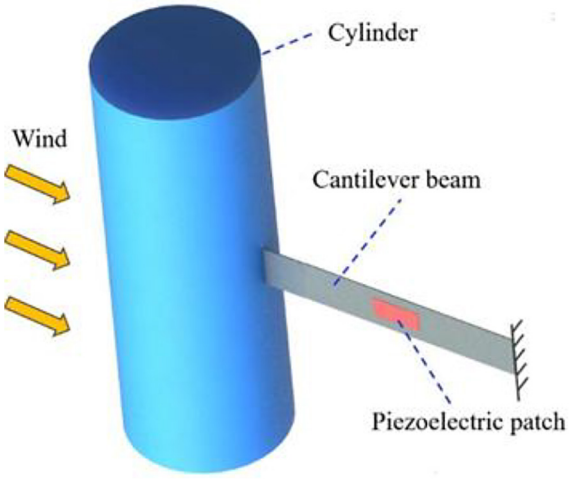

Figure 1. Schematic plot of an aero elastic resonator. Vibration direction (see x in Equation 1) is perpendicular to the direction of wind velocity

electromechanical coupling parameter. The values of system parameters are provided in Table 1. They were adopted from the reference (Li et al., 2024) with further extension with respect to the parameter D. S_t denotes the Strouhal number.

Table 1. System parameters used in calculations

Symbol	Value
m	0.0078 kg
c	0.003 Nsm^{-1}
R	$10^6\,\Omega$
k	26 N/m
D	0.03, 0.06, 0.12, 0.15, 0.18 m
θ	2×10^{-5} N/V
L	0.09 m
C_{l0}, C_{d0}	0.3, 1.2
β, A	0.24, 12
C_p	100 nF
S_t	0.2
ω_s	$2\pi S_t U/D$
ρ	1.2041 kg/m^3

RESULTS AND DISCUSSION

Calculations were done for nodal initial conditions with small offset from zero for q and reported in the steady state limit in Figures 2 and 3. For solving, Wolfram Mathematica and its built-in function NDSolve with automatically chosen solver settings were employed. Nonmonotonic behavior is observed in both displacement and

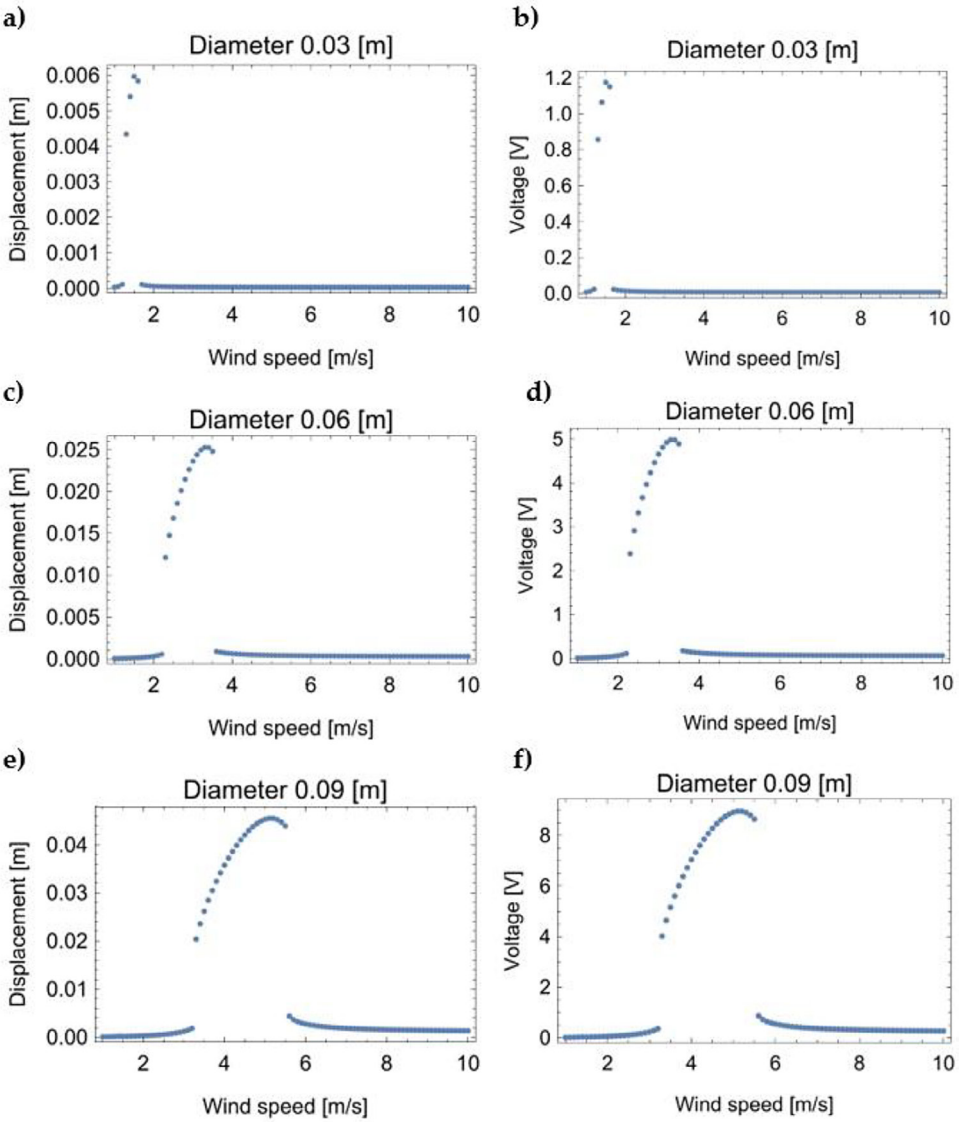

Figure 2. The displacement and voltage (amplitudes) output for increasing diameter D of the cylinder as a function of the wind speed U: (a–b) D = 0.03 m; (c–d) D = 0.06 m; (e–f) D = 0.09 m

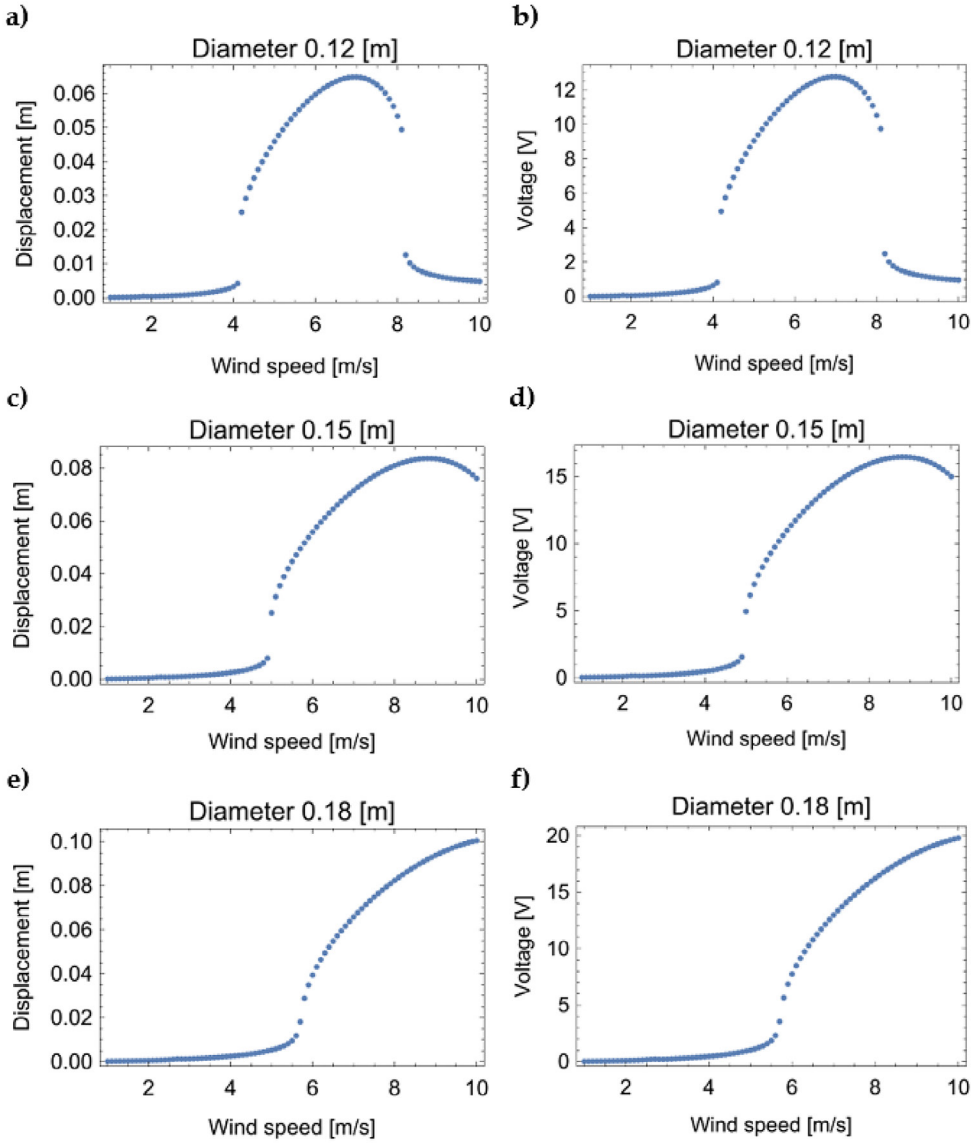

Figure 3. The displacement and voltage (amplitudes) output for increasing diameter D of the cylinder as a function of the wind speed U: (a-b) D = 0.12 m; (c-d) D = 0.15 m; (e-f) D = 0.18 m

voltage amplitude curves versus the wind speed. These two quantities are growing and decreasing together as they are related by the linear coupling (see Equation 3). The rise of the displacement/voltage initiates for very small wind speed U = 0.8 m/s (for D = 0.03 m, see Figure 2ab) and systematically grows with the increasing diameter to U = 5.8 m/s (for D = 0.18 m, see Figure 3ef). Simultaneously, the range of moderate values of displacement and voltage amplitudes as well as the top value are increasing. As far as the voltage output is concerned, the top value starts 1.2 V (for D = 0.03 m) and going across 5.1, 9.0, 13.5, 16.5 (for D: 0.06 m; 0.08 m; 0.12 m; 0.15 m) to reach the maximum 21.0 V (calculated for D = 0.18 m). This is a linear grow. The results of voltage

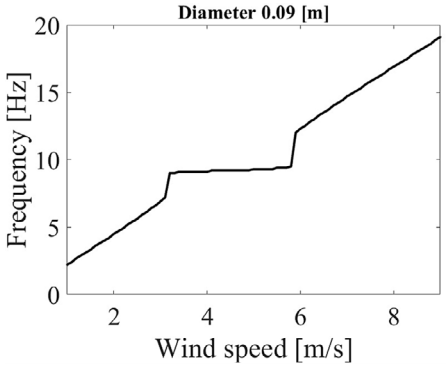

Figure 4. Response vibration frequency as a function of the wind speed for D = 0.09 m. The characteristic plato (reflecting a lock-in phenomenon) indicates output frequency matching with the natural frequency of the mechanical resonator (the bluff-body and elastic suspension) of 9.2 Hz

and displacement amplitude outputs reflect the frequency lock-in phenomenon (Figure 4) as the shedding frequency is fixed (see Equation 3).

It was concluded conclude that the larger diameter (for the constant mass) is useful to provide better performance in the case of variable wind speed. The large range of wind speed is related to nonlinear vortex interaction between the air flow and the mechanical resonator. The obrained results coincide with experimentaly validated case of D = 0.06 m (see Li at al. 2024). Here, the extended studies to the diameter range $D \in [0.03, 0.18]$ m.

Effect of bluff body diameter uncertainty

To examine the uncertainty effect of the bluff body diameter, multiple copies of the system with a small deviation are studied (Li et al., 2019; Kulik et al., 2022; Huang et al., 2020). For simplicity,

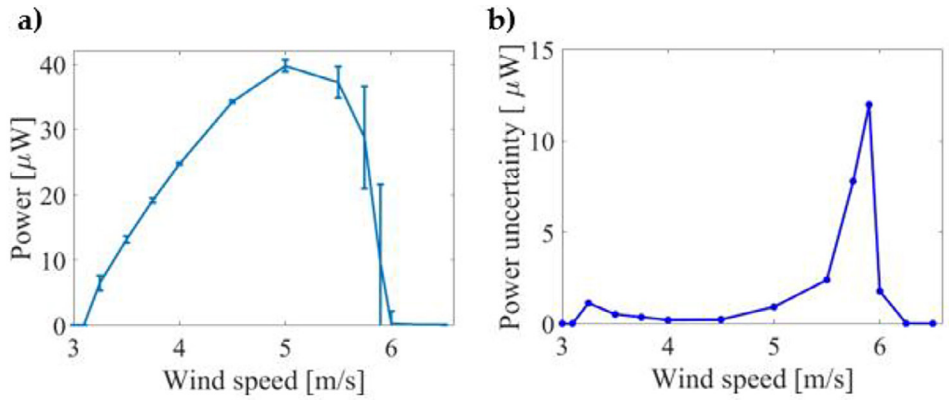

Figure 5. Mean power versus wind speed (a) and its uncertainty (b) for the mean diameter D_0 = 0.09 m and uncertainty σ_D = 0.001 m

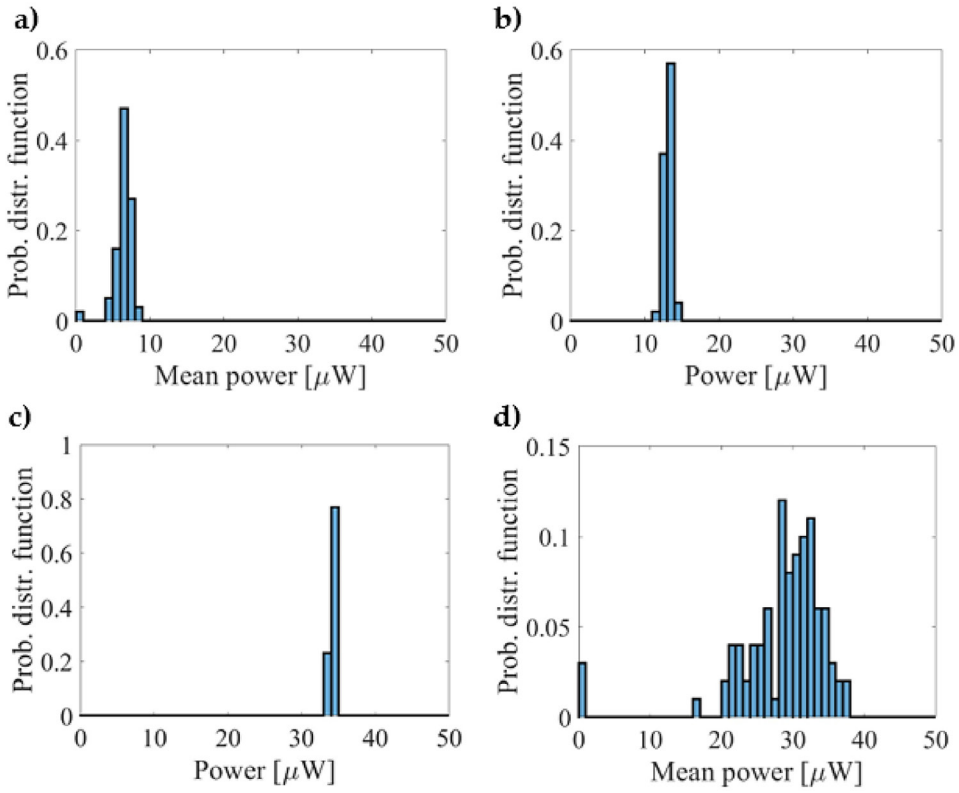

Figure 6. Normalized probability distribution function (pdf) of power output for uncertain diameter the mean diameter D_0 = 0.09 m and uncertainty σ_D = 0.001 m with the wind speed U = 3.25 m/s, 3.5 m/s, 4.5 m/s, 5.75 m/s for (a-d), respectively

the Gaussian distribution of the deviations of the standard deviation σ_D of diameter was assumed around its mean value D_0 and the equations Equations 1–3 were solved multiple times. To obtain good statistics N = 100 copies of the examined system were performed (Figure 1).

The course of the mean power versus wind speed and its uncertainty is shown in Figure 5. The mean power output results for diameter D_0 = 0.09 m and uncertainty σ_D = 0.001 m are presented in Figure 5a. It should be noted that the curve is similar to results of Figure 2f. with the diameter assumed of the same value. Additionally, the uncertainty was observed, expressed as the error bars. For better clarity, they were replotted as the separate function of the wind speed U in Figure 5b). It has the two peaks signaling the stating and finishing the effective mechanism of VIV in the mechanical structure. Figure 6 shows the selected probability distribution functions indicating that for overlapping of solutions (including the nodal solution) caused the increases of discrepancies in power output.

The higher value of uncertainty at the upper edge at U = 5.75 m/s (Figure 6d) is caused by larger slop between the well developed VIV power output and the neighbor bottom response with respect to the lower edge at U = 3.25 m/s (Figure 6a).

CONCLUSIONS

The resonance region is associated with the frequency lock-in phenomena coinciding with the natural frequency of the aero-elastic resonator is strongly dependent on the diameter of the bluff body used. This frequency lock-in region is the most important for VIV energy harvesting. The arguments to select the proper size of the bluff body by increasing its diameter were provided. It could be important to design the system of mistuned bluff bodies (Ahmed et al., 2025). It should be noted that in the performed calculations the mass was fix to the same value despite of the enlarging of the diameter. This is not easy to keep in the real structure. To keep the adequate relation between the mass and diameter, experiments with the styrofoam samples were carried out (Li et al., 2024). In calculation results there was also a an assumption of the fixed approximate shedding frequency. In the next step, the Strouhal number which can slightly change with the flow conditions should be validated by the experiment (Soltani et al., 2023) for any geometrical variation of the bluff body. Power output uncertainty is the principal result of the conducted investigation. It increases rapidly at the edges of VIV mechanism with respect to the bluff body diameter. In the next step system, variable conditions (as the wind speed and direction) will be adopted and considered as uncertain.

Acknowledgements

This research was funded by National Science Centre, Poland under the project SHENG-2, No. 2021/40/Q/ST8/00362.

REFERENCES

1. Ahmed, S.A., Litak, G., Waśkowicz, M., Ravi, D., Giri, A.M., Caban, J. (2025). Response of the air flow energy harvester with two side-by-side bluff-bodies of various shapes. *Journal of Ecological Engineering, 26*, 238–249. https://doi.org/10.12911/22998993/199567
2. Ali A., Ali S., Shaukat H., Khalid E., Behram L., Rani H., Altabey W.A., Kouritem, S.A., Noori M. (2024). Advancements in piezoelectric wind energy harvesting: A review. *Results in Engineering*, *21*, 101777. https://doi.org/10.1016/j.rineng.2024.101777
3. Ambrożkiewicz, B., Czyż, Z., Stączek, P., Tiseira, A., García-Tíscar, J. (2022). Performance analysis of a piezoelectric energy harvesting system. *Advances in Science and Technology Research Journal*, *16*(6), 179–185. https://doi.org/10.12913/22998624/156215
4. Bacinskas, D., Kamaitis, Z., Kilikevicius, A. (2013). A sensor instrumentation method for dynamic monitoring of railway bridges. *Journal of Vibroengineering*, *15*, 176-184.
5. Barta, D., Pavelcik, V., Brezani, M. (2022). Study of air flow around a moving vehicle as a source of energy. *Lecture Notes in Intelligent Transportation and Infrastructure*, *Part F*, 1395, 3–15. https://doi.org/10.1007/978-3-030-94774-3_1
6. Borowiec, M., Gawryluk, J., Bochenski, M. (2021). Influence of mechanical couplings on the dynamical behavior and energy harvesting of a composite structure. *Polymers, 13*, 66. https://doi.org/10.3390/polym13010066
7. Caban, J. (2021). Technologies of using energy harvesting systems in motor vehicles – energy from exhaust system. *20th International Scientific Conference Engineering For Rural Development,* Jelgava, 26–28. 05. 2021, 98–105. https://doi.org/10.22616/ERDev.2021.20.TF020

8. Caban, J., Stączek, P., Wolszczak, P., Nowak, R., Karczmarzyk, S. (2024). Research on the use of multifrequency excitations for energy harvesting in a combustion engine. *Advances in Science and Technology Research Journal*, *18*, 400–412. https://doi.org/10.12913/22998624/190250
9. Camut, J., Müller, E., de Boor, J. (2023). Analyzing the performance of thermoelectric generators with inhomogeneous legs: coupled material–device modelling for Mg2X-based TEG prototypes. *Energies, 16*, 3666. https://doi.org/10.3390/en16093666
10. Ceponis, A., Mazeika, D., Kilikevicius, A. (2019). Bidirectional piezoelectric energy harvester. *Sensors, 19*, 3845. https://doi.org/10.3390/s19183845
11. Chen, Z., Cao, J., Qin, Z., Chen, Z., Xiong, Y. (2022). Simultaneous vibration suppression and energy harvesting of vehicle suspension systems: Status and prospects. *Jixie Gongcheng Xuebao/ Journal of Mechanical Engineering*, *58*, 3–26. https://doi:10.3901/JME.2022.20.003
12. Friswell, M.I., Ali, S.F., Adhikari, S., Lees, A.W., Bilgen, O., Litak, G. (2012). Nonlinear piezoelectric vibration energy harvesting from a vertical cantilever beam with tip mass. *Journal of Intelligent Material Systems and Structures*, *23*(13), 1505–1521. https://doi.org/10.1177/1045389X12455722
13. Gałęzia, A., Gontarz, S., Jasiński, M., Mączak, J., Radkowski, S., Seńko, J. (2012). Distributed system for monitoring of the large scale infrastructure structures based on analysis of changes of its static and dynamic properties. *2nd International Conference on Smart Diagnostics of Structures*, 14–16 Nov. 2011. *Key Engineering Materials*, *518*, 106–118. https://doi.org/10.4028/www.scientific.net/KEM.518.106
14. Gechev, T., Mruzek, M., Barta, D. (2017). Comparison of real driving cycles and consumed braking power in suburban Slovakian driving. *MATEC Web of Conference, 133*, 02003. https://doi.org/10.1051/matecconf/201713302003
15. Giri A.M., Ali S.F., Arockiarajan, A. (2022). Influence of asymmetric potential on multiple solutions of the bi-stable piezoelectric harvester. *European Physical Journal: Special Topics, 231*, 1443–1464. https://doi.org/10.1140/epjs/s11734-022-00496-8
16. Huang D., Zhou S., Han Q., Litak G. (2020). Response analysis of the nonlinear vibration energy harvester with an uncertain parameter. *Proceedings of the Institution of Mechanical Engineers, Part K: Journal of Multi-body Dynamics*, *234*, 393–407. https://doi.org/10.1177/1464419319893211
17. Ikbal, M., Rizal, M., Ali, N., Putra, T.E. (2025). Design and experimental study of piezoelectric energy harvester integrated in rotating vehicle tire using end-cap system. *Results in Engineering, 25*, 104195. https://doi.org/10.1016/j.rineng.2025.104195
18. Jung H., Seung-Woo, L. (2011). The experimental validation of a new energy harvesting system based on the wake galloping phenomenon. *Smart Material Structure, 20*, 55022. https://doi.org/10.1088/0964-1726/20/5/055022
19. Kilikevicius, A., Skeivalas, J., Kilikeviciene, K., Matijosius, J. (2019). Analysis of dynamic parameters of a railway bridge. *Applied Sciences, 9*, 545. https://doi.org/10.3390/app9122545
20. Kim, T., Kim, J., Lee, T.H. (2023). Structure-circuit resistor integrated design optimization of piezoelectric energy harvester considering stress constraints. *Energies, 16*, 3766. https://doi.org/10.3390/en16093766
21. Kindrachuk, M., Volchenko, A., Volchenko, D., Volchenko, N., Poliakov, P., Tisov, O., Kornienko, A. (2019). Polymers with enhanced energy capacity modified by semiconductor materials. *Functional Materials, 26,* 3, 629–634. https://doi.org/10.15407/fm26.03.629
22. Koszewnik, A. (2024). Assessment of parameters of the vibration-based energy harvesting system located in the micro-power generator. *Acta Mechanica et Automatica*, *18*, 223–232. https://doi.org/10.2478/ama-2024-0026
23. Kulik, M., Gabor, R., Jagiela, M. (2022). Surrogate model for design uncertainty estimation of nonlinear electromagnetic vibration energy harwester. *Energies, 15*, 8601. https://doi.org/10.3390/en15228601
24. Labuda, R., Barta, D., Kocalcik, A. (2010). Effective use of the braking effect of vehicle drivetrain at deceleration. *41st International Scientific Conference of Czech and Slovak University Departments and Institutions Dealing with the Research of Internal Combustion Engines (KOKA 2010)*, 206–211.
25. Li, S., Xu, J., Pu, X., Tao, T., Mei, X. (2019). A novel design of a damping failure free energy-harvesting shock absorber system. *Mechanical Systems and Signal Processing, 132*, 640–653. https://10.1016/j.ymssp.2019.07.004
26. Li, Y., Zhou, S., Litak, G. (2019). Uncertainty analysis of excitation conditions on performance of nonlinear monostable energy harvesters. *International Journal of Structural Stability and Dynamics, 19*, 1950052. https://doi.org/10.1142/S0219455419500524
27. Li, Z., Zhang, H., Litak, G., Zhou, S. (2024). Periodic solutions and frequency lock-in of vortex-induced vibration energy harvesters with nonlinear stiffness. *Journal of Sound and Vibrations, 568*, 17952. https://doi.org/0.1016/j.jsv.2023.117952
28. Ma, X., Zhou, S. (2022). A review of flow-induced vibration energy harvesters. *Energy Conversion and Management, 254*, 115223. https://doi.org/10.1016/j.enconman.2022.115223
29. Mhatre, A.S., Shukla, P. (2024). A comprehensive

review of energy harvesting technologies for sustainable electric vehicles. *Environmental Science and Pollution Research*. https://doi.org/10.1007/s11356-024-34865-8

30. Naifar, S., Kanoun, O., Trigona, C. (2024). Energy harvesting technologies and applications for the internet of things and wireless sensor networks. *Sensors, 24(14)*, 4688. https://doi.org/10.3390/s24144688
31. Naik, N., Suresh, P., Yadav, S., Nisha, M.P., Arias-Gonzáles, J.L., Cotrina-Aliaga, J.C., Bhat, R., Jalageri, M.D., Kaushik, Y., Kunjibettu, A.B. (2023). A review on composite materials for energy harvesting in electric vehicles. *Energies, 16*, 3348. https://doi.org/10.3390/en16083348
32. Navrose, Mittal, S. (2019). Intermittency in free vibration of a cylinder beyond the laminar regime. *Journal of Fluid Mechanics, 870*, R2. https://doi.org/10.1017/jfm.2019.310
33. Nowak, R., Pietrzakowski, M. (2016). Experimental and simulation investigations of the cantilever beam energy harvester. *Solid State Phenomena, 248*, 249–255. https://doi.org/10.1177/1687814015627983
34. Nowak, R., Pietrzakowski, M., Rumianek, P. (2020). Influence of design parameters on bending piezoelectric harvester effectiveness: Static approach. *Mechanical Systems and Signal Processing*, *143*, 106833. https://doi.org/10.1016/j.ymssp.2020.106833
35. Soltani, K., Rezazadeh, G., Henry, M.P. (2023). Nonlinear dynamics of a broadband vortex-induced vibration–based energy harwester. *Journal of Engineering Mechanics, 149*, 8, 04023046. https://doi.org/10.1061/JENMDT.EMENG-6898
36. Szumska, E.M., Jurecki, R. (2022). The analysis of energy recovered during the braking of an electric vehicle in different driving conditions. *Energies, 15*, 9369. https://doi.org/10.3390/en15249369
37. Wang, J., Gu, S., Zhang, C., Hu, G., Chen, G., Lai, Y., Yang, K., Li, H., Litak, G., Yurchenko, D. (2020). Hybrid wind energy scavenging by coupling vortex-induced vibrations and galloping. *Energy Conversion and Management*, *213*, 112835. https://doi.org/10.1016/j.enconman.2020.112835
38. Wang, J., Li, G., Zhang, M., Zhao, G., Jin, Z., Xu, K., Zhang, Z. (2018). Energy harvesting from flow-induced vibration: A lumped parameter model. *Energy Sources, Part A*, 40, 2903–2913. https://doi.org/10.1080/15567036.2018.1513100
39. Wang, Y.-P., Chen, W., Huang, Y.-Y., Liu, X., Su, C.-Q. (2022). Performance study on a thermoelectric generator with exhaust-module-coolant direct contact. *Energy Reports, 8*, 729-738. https://doi.org/10.1016/j.egyr.2022.05.228
40. Yang, Z., Zhou, S., Zu, J., Inman, D. (2018). High-performance piezoelectric energy harvesters and their applications. *Joule, 2*, 642–697. https://doi.org/10.1016/j.joule.2018.03.011
41. Yu, R., Feng, S., Sun, O., Xu, H., Jiang, O., Guo, J., Dai, B., Cui, D., Wang, K. (2024). Ambient energy harvesters in wearable electronics: fundamentals, methodologies, and applications. *Journal of Nanobiotechnology*, *22*, 497. https://doi.org/10.1186/s12951-024-02774-0